

# A HIGH-POWER FREQUENCY-STABILIZED TUNABLE TWO-FREQUENCY DIODE LASER SYSTEM FOR GENERATION OF COHERENT TERAHERTZ-WAVE BY PHOTOMIXING

Shuji Matsuura and Geoffrey A. Blake

Division of Geological and Planetary Sciences, California Institute of Technology, Pasadena, CA 91125  
E-mail: matsuura@gps.caltech.edu

Pin Chen

Division of Chemistry and Chemical Engineering, California Institute of Technology, Pasadena CA 91125

J. C. Pearson and Herbert M. Pickett

Jet Propulsion Laboratory, California Institute of Technology, Pasadena, CA 91109

## Abstract

A tunable two-frequency high-power diode laser system at 850 nm for terahertz (THz)-wave generation by photomixing in low-temperature-grown GaAs photo-conductors has been developed. The difference frequency is obtained through a three laser system, where two lasers are locked to different orders of a Fabry-Perot cavity and a third is offset-locked to the first. The difference-frequency signal is generated by the offset laser and the other cavity-locked laser. The spectral purity of the beat note is better than 1 MHz. The maximum output power of ~500 mW was obtained by using the master oscillator power amplifier (MOPA) technique, simultaneous injection of two seed frequencies with a single semiconductor optical amplifier. Here we report the generation of THz waves and spectroscopy of acetonitrile as proof of concept.

## 1. Introduction

The difference-frequency generation, or the frequency down-conversion, by photomixing using nonlinear optical materials and photoconductors has been long investigated as a promising technique to develop widely tunable coherent sources in the terahertz (THz) region. Photomixing in low-temperature-grown (LTG) GaAs photoconductors with

planar antennas is the most attractive method in terms of conversion efficiency<sup>1-3</sup>, and LTG-GaAs photomixer sources have already been applied to laboratory spectroscopy by several authors<sup>4-6</sup>. However, the frequency stability and calibration of these sources have not been sufficient for high-resolution spectroscopic applications. The frequency control and calibration of pump laser system is the key issues for the next generation of such THz sources.

Diode-laser-based systems are suitable for space-borne fiber-coupled instruments because of their compactness, low power consumption, and long lifetime.<sup>2,3</sup> Wide frequency tunability of diode lasers is also an important advantage for applications in the THz-wave generation. The advances in frequency stabilization of diode lasers locked to cavity modes allows us to define the frequency of the THz-wave precisely. We have developed a fiber-coupled, tunable, two-frequency diode laser system at 850 nm using such frequency-stabilization scheme.

The THz-wave output power generated by photomixing with a photoconductor has a quadratic dependence on the photocurrent oscillation induced by the pump lasers. Up to now, the THz-wave output power generated with LTG-GaAs photomixers have been limited to 0.1-1  $\mu$ W level corresponding to the ac-photocurrent of ~0.1 mA, dc-photocurrent of ~1 mA.<sup>6,7</sup> The photocurrent is proportional to the pump laser power, but conventional type

photomixers cannot handle the incident power over ~50 mW because of thermal failure.<sup>7</sup> Large dimension devices allow high-power laser input and provide much higher photocurrent by avoiding the thermal problem. In order to drive these devices, the development of high-power (>>50 mW) tunable diode laser is required. Unfortunately, the output power of our fiber-coupled diode laser system was not sufficient for this purpose.

The master oscillator power amplifier (MOPA) technique solve the dilemma between narrow linewidth and high power. The master laser with narrow linewidth is injected into the power amplifier, and the laser power is amplified while preserving the spectral purity. Although the MOPA has been normally used for single-frequency operation, simultaneous two-frequency injection seeding to a single power amplifier is achievable<sup>8</sup>. The two-frequency MOPA operation has an advantage

in spatial overlap of the two frequency beams, which is essential to achieve an efficient photomixing.

We developed a high-power, narrow-linewidth, tunable two-frequency diode laser system at 850 nm based on the two-frequency MOPA with the fiber-coupled tunable master laser and a single optical amplifier. In this paper, design and performance of this system and its application to the THz-wave generation and spectroscopy are presented.

## 2. Laser system design and performance

### 2-1. Frequency-stabilized tunable diode laser

The fiber-coupled tunable two-frequency diode laser system to synthesize a precise difference-frequency consists of three external

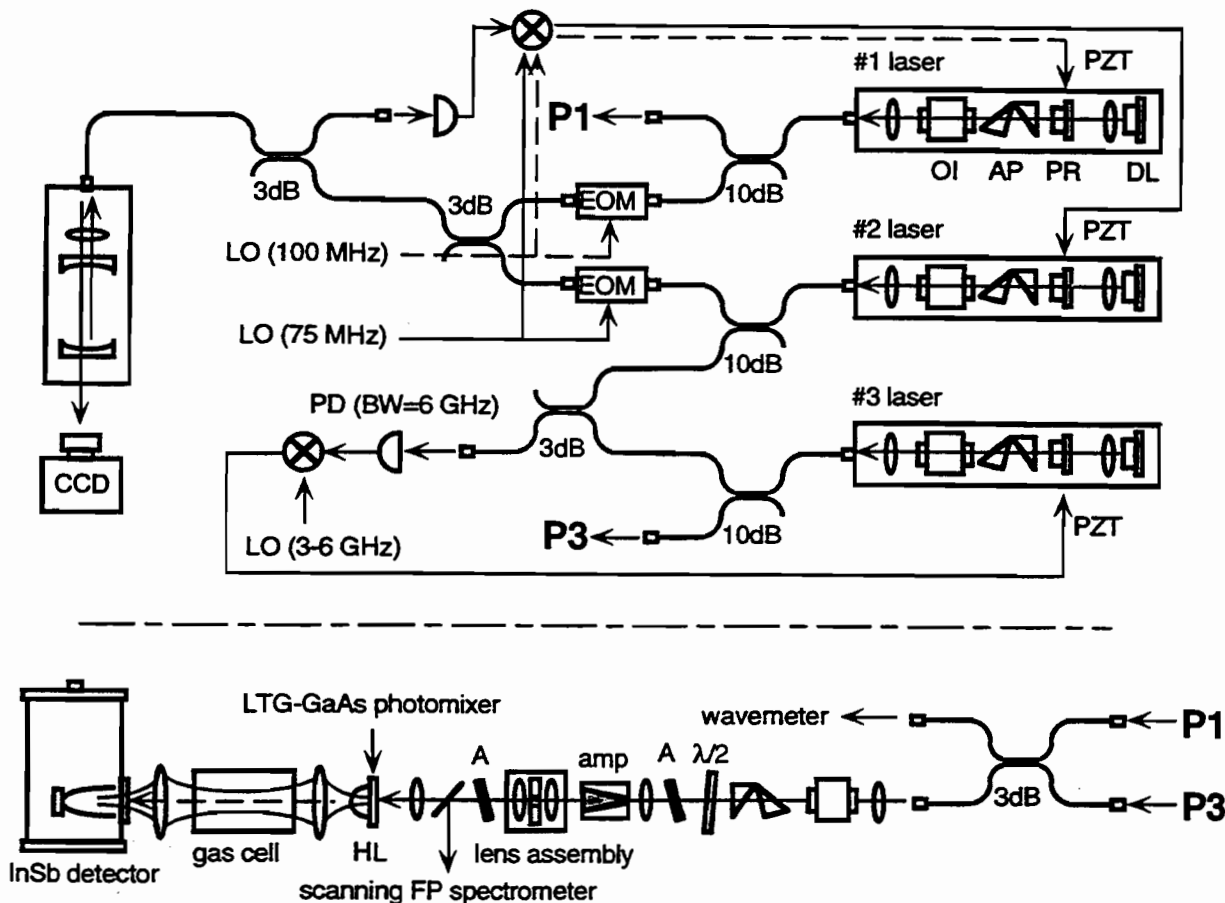


Fig. 1: Schematic diagram of the laser system and experimental setup of the spectroscopy. DL, DBR diode laser; PR, partial reflector; AP, anamorphic prism pair; OI, optical isolator;  $\lambda/2$ , half-wave plate; A, attenuator; HL, hyper-hemispherical lens; PD, photodetector.

cavity diode lasers as depicted in Figure 1. Two of these lasers (#1 and #2) are locked to different longitudinal modes of a Fabry-Perot (FP) cavity with a free spectral range (FSR) of 3 GHz. The third laser (#3) is locked to one of the cavity-locked lasers (#2) with a 3-6 GHz tunable offset, which can be continuously swept over the FSR. The difference frequency between the #1 and #3 is precisely determined by the sum of integral multiples of the FSR and the offset frequency. All the components are connected with single-mode polarization-maintained fiber optics.

Each external cavity laser assembly consists of an 852 nm distributed Bragg-reflector (DBR) semiconductor laser diode (SDL5722), an  $f=4$  mm collimating lens, a 20% partial reflector mounted on piezoelectric transducer (PZT), an anamorphic prism pair, a 60-dB optical isolator, an  $f=4$  mm focusing lens, and a FC-connecterized fiber mount. These components were assembled in an aluminum rail assembly as shown in Figure 1. The temperature of the diode laser is controlled by a thermo-electric (TE) cooler with an accuracy better than 1 mK. The injection current is supplied by a low noise ( $7 \text{ nA}/\sqrt{\text{Hz}}$ ) current driver. The partial reflector and the DBR in the laser chip constitute an external cavity with FSR of  $\sim 3$  GHz. The optical feedback induced by the external cavity narrows the linewidth of  $\sim 500$  kHz, while typical linewidth of DBR lasers is several megahertz. The laser frequency was continuously tunable within the FSR of the external laser cavity by changing the cavity length. The continuous tunable range could be expanded to 5 GHz, which corresponds to the voltage limit applied to the PZT ( $\pm 15$  V), by tracking the laser temperature to maximize the laser gain at the external cavity mode frequency.

To improve the long-term frequency stability, the laser frequency was locked to longitudinal modes of the ULE (Ultra Low Expansion:  $\alpha = -2 \times 10^{-10} \text{ }^\circ\text{C}^{-1}$ ) FP-cavity with a finesse of 750 and FSR of 3 GHz. The FP-cavity is installed in a sealed box filled with dry nitrogen to prevent from refractive index change caused by variations in surrounding pressure. To lock the laser frequency to the FP-cavity mode, we used the Pound-Drever-Hall method. The FM sidebands of the laser are generated at  $\sim 100$  MHz with a fiber-coupled electro-optic phase modulator (EOM), and the

modulated signal is injected into the FP-cavity. The reflected signal from the FP-cavity is detected and fed back to the PZT of the laser cavity. The feedback loop bandwidth was limited to 500 Hz by acoustic resonance of the PZT. The dc-drift of the frequency caused by thermal expansion of the external laser cavity is canceled by tracking the PZT voltage with the integrated error signal through the computer control system. In the laboratory environment the drift was so large that the feedback voltage to the PZT reaches to the 15-V limit in a few minutes. The drift was considerably reduced by putting the whole laser system on a temperature-controlled thick aluminum plate, and the all-day-long cavity-lock of the laser frequency was achieved.

Combined output power of the #1 and #3 lasers from the final 3-dB fiber coupler was approximately 30 mW, while the output power of each DBR laser was originally 150 mW. The total power loss of the present system consisted of the transmission loss in the free-space optics in the laser assembly (1.5dB), the insertion loss to the fiber (4dB), and the loss in fiber directional couplers and at fiber connectors (1.5dB).

## 2-2. Two-frequency MOPA system

The two-frequency MOPA system was constructed using a single traveling-wave 850 nm semiconductor tapered optical amplifier, which was a component of a commercial external-cavity single-mode laser (SDL8630). The two-frequency fiber-coupled output beam from the tunable laser system, a master oscillator, is launched into the free-space through a collimating lens. The circular beam passed through an optical isolator and a half-wave plate for fine adjustment of the polarization, and is reshaped to elliptical beam by an anamorphic prism pair to match the spatial mode to the amplifier facet spot. After appropriate attenuation, the beam is injected into the optical amplifier chip through an  $f=8$  mm focusing lens. The output beam from the amplifier is spatially filtered and collimated to  $\sim 3$ -mm size Gaussian beam by a lens assembly. After passing through an attenuator and a beam divider for monitoring the spectrum, the beam is focused on the photomixer.

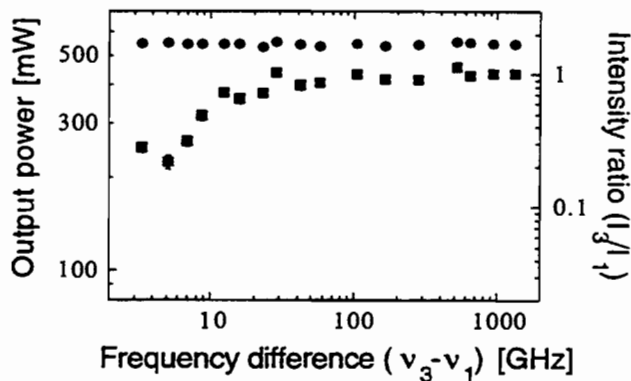


Fig. 2: The output power of the laser system (circles) and the intensity ratio between the two frequency components (squares) as a function of the difference frequency.

Under the conditions of the temperature of 22 °C and the injection current of 1.9 A, the optical amplifier provides the saturated output power of ~500 mW for the input power of approximately 4 mW. Since we set the input power to ~10 mW, the amplifier was operated under highly saturated conditions. Therefore, the output power is insensitive to the input power and the frequency.

### 2-3. Spectral properties

In Figure 2 the amplified output power as a function of the frequency difference between #1 and #3 lasers is shown by the circles. According to the highly saturated condition, the output power was constant within 5% over the entire difference frequency range.

The intensity ratio between the two frequency components in the amplifier output,  $I_3/I_1$ , measured with a scanning FP-spectrometer is also plotted in Figure 2 as a function of the difference frequency. The intensity ratio was close to unity over a wide range of difference frequencies from ~10 GHz to 1.3 THz. Unbalanced amplification occurred at difference frequencies lower than 10 GHz due to the two-frequency interaction driven by the refractive index change induced by the carrier density modulation at the difference frequency<sup>7</sup>. The lower frequency limit of the well-balanced two-frequency amplification is determined by the carrier lifetime of the

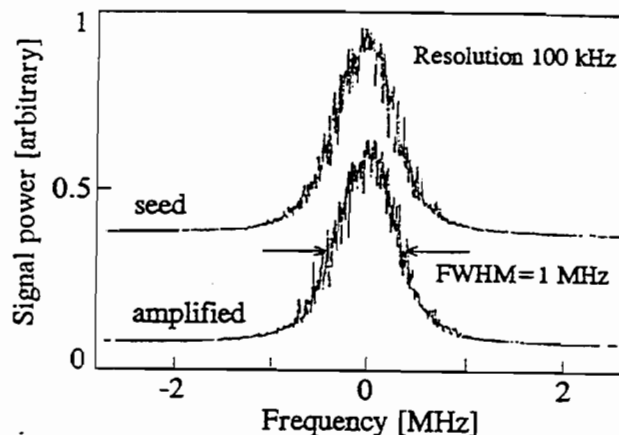


Fig. 3: The spectrum of the beat signal between the two frequency components before amplification (upper) and after amplification (lower).

amplifier.

Since the amplifier used in this system is a component of a commercial external-cavity single-mode laser, an amplifier chip facet was anti-reflection coated ( $R=0.1\%$ ) but the other facet was not coated ( $R=30\%$ ). Small variation in the output power and the intensity balance seen in Figure 2 are caused by the chip mode with a spacing of ~15 GHz. Therefore, these frequency dependence can be considerably reduced by AR-coating both of the amplifier chip facets.

The spectral purity of the beat signal at the difference frequency was measured with the 25-GHz bandwidth photodetector. Figure 3 represents the beat signal spectrum at 12.6 GHz for both the amplified output and the master laser. The linewidth of the beat signal was approximately 1 MHz and completely preserved through the amplification process.

## 3. Generation of THz-wave and application to spectroscopy

### 3-1. Experimental setup

The laser system described above was used for the THz-wave generation with a LTG-GaAs photomixer, and the absorption spectroscopy of acetonitrile ( $\text{CH}_3\text{CN}$ ) was carried out using this THz source. The experimental setup of the spectroscopy is shown in Figure 1. The two-frequency output

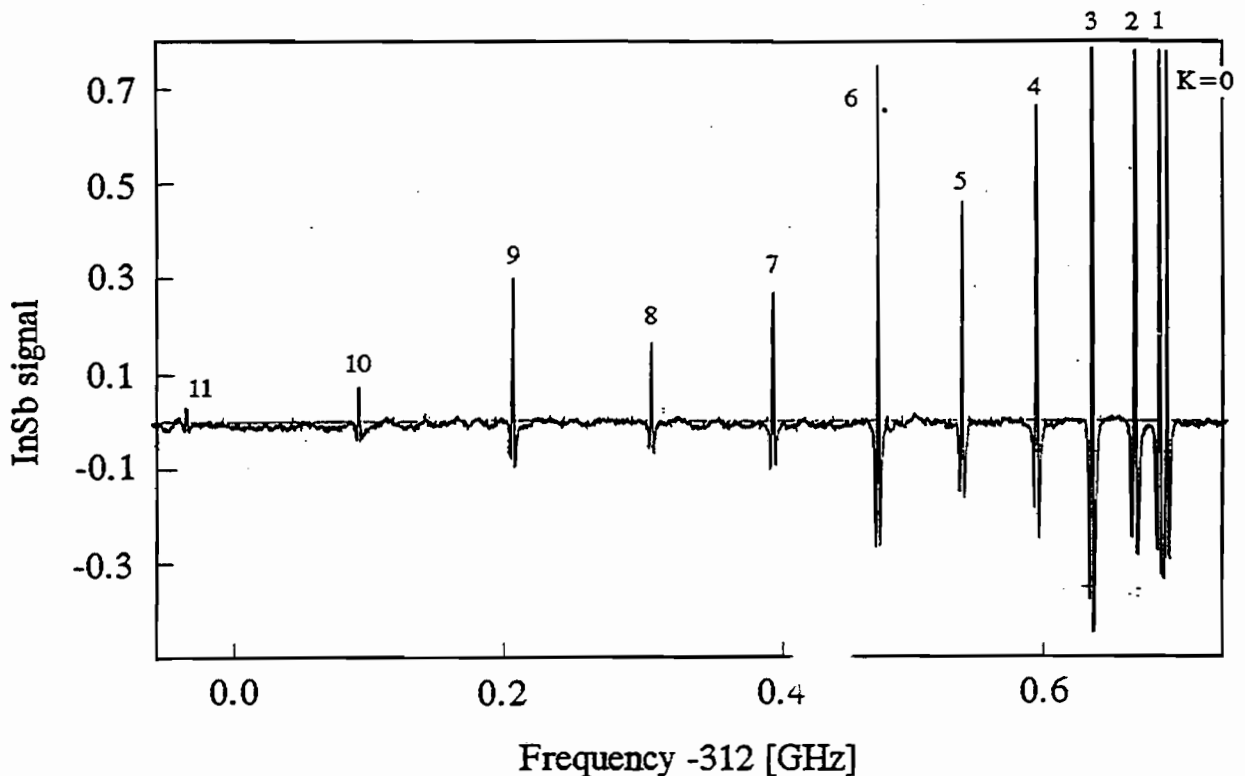


Fig. 4: The measured rotational spectrum of acetonitrile.

beam from the MOPA is attenuated and focused on the LTG-GaAs photomixer. The THz-wave output beam is collimated with a combination of a hyper-hemispherical lens put on a backside of the photomixer and a Teflon lens. The collimated beam passes through a 8-cm long 1-inch diameter gas cell with polyethylene windows. The transmitted beam was weakly focused with a Teflon lens and fed into a 4.2-K InSb hot-electron bolometer.

### 3-2. Generation of THz-wave by photomixing

The photomixer used in this experiment was fabricated at Minnesota University. The LTG-GaAs wafer was grown on a 0.5-mm-thick semi-insulating GaAs substrate, and a planer log-spiral antenna with 1- $\mu\text{m}$ -wide interdesitated electrodes and 1- $\mu\text{m}$ -wide gaps in a  $10 \times 10 \mu\text{m}^2$  active area was etched on the wafer. The bandwidth of the photomixer determined by a combination of the carrier

lifetime of the LTG-GaAs and the RC time constant of the electrode is estimated to be approximately 300 GHz. The dc bias voltage was applied to the electrode by a constant current supply of  $\sim 0.5$  mA for the laser power of 30 mW.

Before carrying out the spectroscopy, the THz-wave power was measured without the gas cell. The pump laser beam was modulated at 400 Hz by a mechanical chopper, and the output signal of the InSb detector was measured. The  $\times 100$ -amplified detector signal at 300 GHz was  $\sim 100$  mV that corresponds to the radiation power of  $\sim 1 \mu\text{W}$ .

### 3-3. Spectroscopy

The tone-burst FM spectroscopy method<sup>9</sup> was used to obtain the spectrum. The injection current of the #1 cavity-locked laser of the master laser system was modulated at 2 MHz above the cavity-lock loop bandwidth, and the

modulation input was switched on and off at a 10-kHz rate. The detected signal was demodulated by a lock-in amplifier at 10-kHz switching rate. The spectrum was obtained by sweeping the offset frequency. The lock-in signal traces the second derivative of the absorption spectrum.

Figure 4 presents the absorption spectrum of  $\text{CH}_3\text{CN}$   $J=16$  rotational transitions near 312 GHz. The lock-in amplifier signal taken by a single frequency sweep with a rate of 2 MHz/sec was plotted against the offset frequency between #2 and #3 lasers. The data sampling rate was 7 sample/sec which corresponds to the frequency resolution of 0.3 MHz, while the time constant of the lock-in amplifier was 0.3 sec. The spectrum shows a  $K$ -structure of a symmetric-top molecule that was assigned to  $K=0-11$  lines as depicted in the figure. The  $K=0$  and 1 lines separated by  $\sim 6$  MHz are clearly resolved. The width of the absorption lines was pressure-limited, while the gas pressure was 60 mTorr. To evaluate the instrumental linewidth, further measurements by changing the gas pressure are required.

The lock-in amplifier outputs for the absorption lines were  $\sim 100$  mV, while the noise amplitude was  $\sim 5$   $\mu\text{V}_{\text{p-p}}$ , and the detection limit of the absorption is estimated to be  $\sim 10^{-4}$ . The spectrum of the  $\text{C}^{13}$ -isotopomer of acetonitrile, which has the natural abundance of  $\sim 1\%$ , was detected with a signal-to-noise ratio of  $\sim 20$  according to the detection limit. Unfortunately, the noise originated mainly from an electronic pick-up at the A/D input, and the detection limit was determined by neither the detector noise nor the source noise. The detection limit of  $10^{-5}$  level can be achieved with the present system by reducing this noise. Although the present measurement was carried out at  $\sim 300$  GHz, the source intensity is sufficiently high for the spectroscopy at higher frequencies if only the detector is replaced to that for high-frequency use; the output power at 1 THz is estimated to be  $\sim 10$  dB down.

For further spectroscopic measurements such as the search for unknown molecular lines and the use for astronomical observation, the absolute frequency calibration of the system is necessary. The frequency calibration is carried out by measuring the FSR of the FP-cavity. Once the exact value of the FSR was obtained, the THz-wave frequency can be determined

with an accuracy of  $\sim 10^{-10}$ , even if there exists a fluctuation of the cavity temperature of  $\sim 1$  °C, because of an extremely low thermal expansion coefficient of the cavity material which is equivalent to the crystal used as a microwave oscillator. The FSR was measured by detecting the beat signal between the two cavity-locked lasers (#1 and #2). The accuracy of the measurement was  $\sim 10$  kHz, while the FSR is 3 GHz. Well-known strong molecular lines in the THz region such as rotational transitions of carbon monoxide (CO) are usable for more accurate calibration. Frequencies of such molecular lines in the THz range that corresponds to  $\sim 300$  times of the FSR are known with an accuracy of  $\sim 10^{-7}$ , and the resultant accuracy of the FSR measurement is expected to be  $\sim 3 \times 10^{-10}$  or  $\sim 300$  Hz. The cavity calibration with CO lines is in the process.

#### 4. Conclusions

A 850 nm tunable two-frequency diode laser system based on the three-laser frequency control scheme and the two-frequency MOPA technique was developed, and the output power of 500 mW and the linewidth of  $< 1$  MHz were achieved. The laser system was applied to the THz-wave generation using the LTG-GaAs photomixer, and the absorption spectroscopy of acetonitrile with this source was demonstrated. The present THz-wave source system is usable for actual spectroscopy, only if the frequency calibration is carried out. The system will be useful not only for spectroscopy but also for the application in development of local oscillators for future space-borne heterodyne receivers.

The photomixer used in the present experiment provided the output power of  $\sim 1$   $\mu\text{W}$  for the pump laser power of 30 mW. According to a straightforward calculation by the quadratic dependence of the THz-wave power on the pump laser power, the sub-mW level output power is achievable by using the present laser system with the maximum power of 500 mW. In order to use such high-power laser effectively, the development of new type of the photomixer with high thermal-damage threshold such as the large dimension device is required.

Since the gain bandwidth of the semiconductor optical amplifier is over 10 THz, the two-frequency MOPA system is applicable to the difference-frequency generation of the mid-infrared radiation. At higher frequencies, even at several THz, the optical down-conversion method using nonlinear optical materials<sup>10</sup> or recently developed quantum-well devices could be more efficient than the electro-optical conversion method using the photomixer. Further development of nonlinear optical materials and novel devices with large  $\chi^{(2)}$  at the diode laser frequency and the phase matching condition at the THz frequency is expected.

We thank T. J. Crawford of Jet Propulsion Laboratory for his technical support. This work was supported by the National Aeronautics and Space Administration.

## References

1. E. R. Brown, K. A. McIntosh, K. B. Nichols, O. B. McMahon, W. F. DiNatale, and T. M. Lyszczarz, *Appl. Phys. Lett.* **67**, 3844 (1995).
2. K. A. McIntosh, E. R. Brown, K. B. Nichols, and C. L. Dennis, *Appl. Phys. Lett.* **66**, 285 (1995).
3. S. Matsuura, M. Tani, and K. Sakai, *Appl. Phys. Lett.* **70**, 559 (1997).
4. A. S. Pine, R. D. Suenram, E. R. Brown, and K. A. McIntosh, *J. Mol. Spectrosc.* **175**, 37 (1996).
5. P. Chen, G. A. Blake, M. C. Gaidis, E. R. Brown, K. A. McIntosh, S. Y. Chou, M. I. Nathan, and F. Williamson, *Appl. Phys. Lett.* **71**, 1601 (1997).
6. S. Matsuura, M. Tani, H. Abe, K. Sakai, H. Ozeki, and S. Saito, *J. Mol. Spectrosc.* **187**, 97 (1998).
7. S. Verghese, K. A. McIntosh, and E. R. Brown, *IEEE Trans. Microwave Theory and Tech.* **45**, 1301 (1997).
8. S. Matsuura, P. Chen, G. A. Blake, J. C. Pearson, and H. M. Pickett, *Opt. Lett.*, submitted.
9. H. M. Pickett, *Appl. Optics* **19**, 2745 (1980).
10. Y. R. Shen, *The Principles of Nonlinear Optics* (John Wiley and Sons, 1984).